A Clinical Application of Ensemble ICA to the Quantification of Myocardial Blood Flow in Dynamic $H_2^{15}O$ PET

Byeong Il Lee[†], Jae Sung Lee[†], Dong Soo Lee[†],
Won Jun Kang[†], Jong Jin Lee[†], Seungjin Choi[§]

[†] Department of Nuclear Medicine
Seoul National University College of Medicine, Korea

[§] Department of Computer Science
Pohang University of Science and Technology
San 31 Hyoja-dong, Nam-gu
Pohang 790-784, Korea
Tel: +82-54-279-2259
Fax: +82-54-279-2299
Email: seungjin@postech.ac.kr

Corresponding author: Seungjin Choi
seungjin@postech.ac.kr

Revised, April 17, 2007

submitted to a special issue of data fusion
Journal of VLSI Signal Processing Systems

Abstract

Ensemble independent component analysis (ICA) is a Bayesian multivariate data analysis method which allows various prior distributions for parameters and latent variables, leading to flexible data fitting. In this paper we apply ensemble ICA with a rectified Gaussian prior to dynamic $H_2^{15}O$ positron emission tomography (PET) image data, emphasizing its clinical usefulness by showing that major cardiac components are successfully extracted in an unsupervised manner and myocardial blood flow can be estimated in 15 among 20 patients. Detailed experiments and results are illustrated.

Keywords: Bayesian learning, Independent component analysis (ICA), Myocardial blood flow quantification, Positron emission tomography (PET).

1 Introduction

The dynamic $H_2^{15}O$ cardiac positron emission tomography (PET) has been widely used for the quantification of myocardial blood flow (MBF) [1, 17, 8, 7, 9, 21], since $H_2^{15}O$ is an ideal blood flow tracer, which is freely diffusible and has stable characteristics. The half life of $H_2^{15}O$ is about 2 minutes, which makes repetitive (more than 2 or 3 times) and short interval estimation (every 10 minutes) of MBF possible. It is essential to extract the left ventricle input function for the calculation of MBF in the tracer kinetics model of dynamic $H_2^{15}O$ cardiac PET. However, it is required to carefully determine the region of interest (ROI) for the precise extraction of the input function, which is not an easy task because of the partial volume effect resulting from the limitation of system resolution and the spill-over of left ventricle, right ventricle and myocardium caused by the motion of heart. Consequently, a new method for the input function extraction is required to estimate the blood flow more accurately.

Linear model-based methods, including factor analysis, principal component analysis (PCA), independent component analysis (ICA) and nonnegative matrix factorization (NMF) methods, have been used for the extraction of input function [1, 17, 15, 14]. In the framework of linear

models, the goal is to learn basis vectors and associated encoding variables (latent variables), given a set of data samples. When a linear model-based method is applied to the dynamic $H_2^{15}O$ cardiac PET, what are expected as successful results, are as follows. Learned basis vectors are associated with the time-activity curves (TACs) which reflect activities of cardiac components across the time and encoding variables correspond to major cardiac components such as left ventricle, right ventricle, and myocardium.

Factor analysis assumes that encoding variables (that are known as factors in this case) follow mutually independent Gaussian distributions and uncertainty (noise) is also Gaussian and independent thereof. Under these assumptions, factor analysis finds a linear model that best models the covariance structure of the data. PCA is closely related to factor analysis, the goal of which is to determine principal directions that are associated with the largest eigenvectors of the data covariance matrix. In contrast to factor analysis and PCA that are based on 2nd-order statistics, ICA exploits either higher-order statistics or non-Gaussianity for data fitting, assuming that latent variables are non-Gaussian as well as mutually independent, ICA finds a linear model by maximizing the output entropy or minimizing the mutual information between output variables. Various methods for ICA have been extensively developed. For example, see [6, 4, 3] for reviews of ICA. Factor analysis and ICA were shown to be useful in extracting cardiac components from dynamic $H_2^{15}O$ cardiac PET [1, 17]. However, these methods often produce negative values in a learned TAC, which is not desirable. On the other hand, nonnegative matrix factorization (NMF) [12] imposes nonnegativity constraints on both basis vectors and encoding variables. NMF was successfully applied to dynamic $H_2^{15}O$ cardiac PET [15, 14], avoiding any negative values in a learned TAC.

Ensemble ICA [19] is a Bayesian ICA where the linear generative model for ICA is optimized over a parametric distribution that approximates the intractable true posterior distribution.

Allowing various prior distributions for parameters and latent variables, leads to more flexible data fitting and source separation. The main benefit of ensemble ICA over factor analysis, ICA, and NMF, is its flexibility since various prior distributions for model parameters allow data fitting as well as learning. With a rectified Gaussian prior, ensemble ICA seeks independent and nonnegative components, which is desirable in our task. In this paper we apply ensemble ICA to $H_2^{15}O$ cardiac PET images that are acquired from 20 patients, in order to estimate MBF. In contrast to our previous study involving PET scan of heart activity of dogs [1, 17, 14], we investigate the usefulness of ensemble ICA in analyzing clinical data acquired from patients, showing that ensemble ICA is a promising tool for medical image analysis. In this paper we include more clinical study, elaborating further our earlier work [11] where ensemble ICA was first applied to PET image data.

The rest of the paper is organized as follows. The next section describes details on experiments and methods, such as PET image acquisition, image processing and analysis methods, a quantification method involving regional myocardial blood flow (rMBF), and so on. Sec. 3 illustrates the clinical results with PET images acquired from 20 patients. Finally conclusions are drawn in Sec 4 with a discussion of the results.

2 Materials and Methods

2.1 Materials

Dynamic $H_2^{15}O$ myocardial PET was performed on 20 patients (15 male subjects that are 55 $\pm$10.8 years old and 5 female subjects that are 64 $\pm$2.9 years old) who underwent gated ^{99m}Tc-MIBI myocardial perfusion SPECT for the suspicious coronary artery disease. Images were acquired at rest and during adenosine stress. Nine of the patients underwent angiography (3

vessels for 4 subjects, 2 vessels for 3 subjects, and 1 vessel for 2 subjects).

2.2 SPECT and PET image acquisition

Gated myocardial SPECT images were acquired using the dual head SPECT camera (Vertex EPIC, Philips-ADAC Labs, Milpitas, USA) with low energy high collimator. Images were reconstructed using the filtered back projection method with ramp filter and butterworth(cutoff frequency=0.33, degree=5) filter. ECAT EXACT47 (Siemens-CTI, Knoxville, USA) was used for PET image acquisition. Transmission scan was performed during 4 minutes using 68Ga/69Ge, and emission scan was performed at rest and adenosine stress state respectively. Totally 24 frames with 47 transaxial images were acquired; 12 frames for 5 seconds, 9 frames for 10 seconds, and 3 frames for 30 seconds. After bolus injection of $H_2^{15}O$ (555-740 MBq), adenosine stress was carried out during 7 minutes. $H_2^{15}O$ was injected after 3 minutes during stress, and then dynamic PET images were acquired during 4 minutes continuously. Images were reconstructed using FBP (image matrix = 128 $\times$ 128, magnification factor = 1.5)

2.3 Image processing

Because of a lot of background of dynamic heart image, all frame data was summed to make a static image for axis reorientation. With this static image, short axis was determined for the transformation of short axis image before summing the slices to increase the SNR of the images. Determined short axis was applied to dynamic data reversely for transformation of all dynamic data. Two planes of short axis images were summed in order to extract myocardium component automatically using ensemble ICA (see Fig. 1). FIRE (Functional Image REgistration) software was used for axis reorientation [18, 10], and ensemble independent component separation and myocardial blood flow estimation was tested using Matlab software. Nine regions of interest

(ROI) were drawn manually on left ventricle and myocardium (1 apex, 4 middle wall, 4 basal wall) to take out the time-activity curve of dynamic PET image. Using the input function and time-activity curve of each region, rMBF was calculated. The values of rMBF were compared with angiography and gated myocardial perfusion SPECT. Regional perfusion was relocated to the 9 regions used above in dynamic PET analysis.

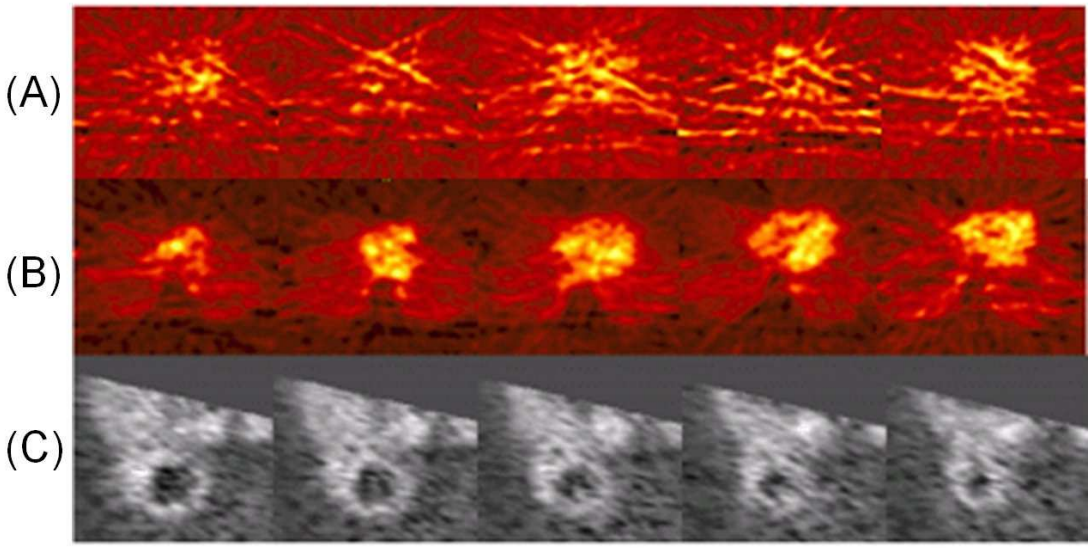

Figure 1: (A) Dynamic $H_2^{15}O$ PET image acquired using ECAT ECAT47 scanner. (B) Summed static image. (C) Tissue component image obtained using ensemble ICA in this study (the image was transformed to the short axis). Noise is present in dynamic image data (as shown in (A) and static image data (as shown in (B)). However, component images (as shown in (C)) extracted by ensemble ICA clearly show myocardium.

2.4 Separation of factor images using ensemble ICA

$H_2^{15}O$ PET images are converted to vector sequences $\mathcal{D} = \{x_t \in \mathbb{R}^m\}$. ICA assumes that data vectors x_t are generated by

$$x_t = As_t + \epsilon_t, \tag{1}$$

where $s_t \in \mathbb{R}^n$ correspond to factor images (independent components), column vectors of the matrix $A \in \mathbb{R}^{m\times n}$ represent time activity curves, and $\epsilon_t \in \mathbb{R}^m$ reflect the model uncertainty which is assumed to be Gaussian.

In the context of $H_2^{15}O$ PET images, the independent components that are expected to appear correspond to left ventricle, right ventricle, myocardium, and background, which reasonable satisfy spatial independence. In such a case, basis vectors (corresponding to the column vectors of A) represent the time activity curves which reflect the time-varying influence in PET images [21]. Standard ICA, including mutual information minimization, maximum likelihood estimation (MLE), output entropy maximization, and so on (see [3] for recent review), takes into account the prior probability of parameters in a limited way and neglects the uncertainty term in (1). In standard ICA, parameters are inferred by maximizing the likelihood in the limit of zero noise.

On the other hand, NMF [12] also considers the linear model (1) but infers parameters through constraining both A and s_t to be nonnegative, whereas ICA imposes independence conditions for s_t. Inference in NMF can also be illustrated in the framework of maximum likelihood estimation, assuming Poisson distribution for ϵ_t [12]. Application of NMF to dynamic PET can be found in [14].

Here we use ensemble ICA [19] to extract factor images in $H_2^{15}O$ PET. In the Bayesian framework, the posterior probability of parameters Θ, given a set of data points $\mathcal{D}$, is described by

$$P(\Theta|\mathcal{D},\mathcal{H}) = \frac{P(\mathcal{D}|\Theta,\mathcal{H})P(\Theta|\mathcal{H})}{P(\mathcal{D}|\mathcal{H})}, \tag{2}$$

where $\mathcal{H}$ represents a model. In ensemble learning, the inference is performed by averaging over the posterior distribution, so that the inference is sensitive to regions where the probability mass is large, in contrast to ML or MAP where the inference is sensitive to regions where the

probability density is large. In practice, exact inference is often intractable. Ensemble learning finds an approximate posterior distribution Q for the model parameters by minimizing the Kullback-Leibler divergence between the approximate posterior Q and the true posterior

$$\begin{aligned} KL[Q||P] &= \left\langle \log\left[\frac{Q(\Theta)}{P(\Theta|\mathcal{D},\mathcal{H})}\right]\right\rangle_Q \\ &= \left\langle \log\left[\frac{Q(\Theta)}{P(\mathcal{D},\Theta|\mathcal{H})}\right]\right\rangle_Q + \log P(\mathcal{D}|\mathcal{H}). \end{aligned} \tag{3}$$

where $\langle\cdot\rangle_Q$ denotes the statistical expectation under an approximate distribution Q.

The following objective function $\mathcal{J}$ was considered in [19]

$$\begin{aligned} \mathcal{J} &= KL[Q||P] - \log P(\mathcal{D}|\mathcal{H}) \\ &= \left\langle \log\left[\frac{Q(\Theta)}{P(\mathcal{D},\Theta|\mathcal{H})}\right]\right\rangle_Q \\ &\geq -\log P(\mathcal{D}|\mathcal{H}). \end{aligned} \tag{4}$$

The minimization of the objective function $\mathcal{J}$ in (4) is equivalent to maximizing the lower-bound on the log-evidence $\log P(\mathcal{D}|\mathcal{H})$.

For tractable calculation, the approximate posterior distribution $Q(\Theta)$ is assumed to be of factorized form,

$$Q(\Theta) = Q(s)Q(\theta), \tag{5}$$

where s represents latent variables and θ is a collection of model parameters as well as hyper-parameters. Each $Q(s)$ and $Q(\theta)$ is further factorized, depending on parameters. Ensemble learning (or variational Bayesian learning) determines $Q(s)Q(\theta)$ iteratively through EM-like optimization where the variational E-step determines $Q(s)$ which minimizes (4) given $Q(\theta)$ and the variational M-step finds $Q(\theta)$ which minimizes (4) given $Q(s)$. Detailed algorithms can be found in [19].

The main benefit of ensemble ICA is to decompose the PET images as a linear combination of factor images with encoding variables being statistically independent as in ICA, while imposing nonnegativity constraints on A and s_t through the rectified Gaussian prior. In other words, ensemble ICA allows us to incorporate both independence and nonnegativity constraints in the context of the linear model (1).

2.5 Quantification method

Perfusion information of rest and stress state in gated myocardial perfusion SPECT and diagnosis results of angiography which were expressed as percentage according to territory were used for this study. Correlation was evaluated between 9 regions for the measurement of rMBF twice. The rMBF from $H_2^{15}O$ dynamic myocardial PET were compared with the results of angiography and perfusion SPECT. And image contrast between myocardium and left ventricle was estimated in segmented myocardial independent component images.

2.6 Analysis of PET blood flow as the result of angiography

Stenosis of angiography is defined as ratio of narrowing diameter by intact diameter. From the result of angiography, regions were divided according to their degree of stenosis (50%). The regional SPECT perfusion and absolute blood flow of PET were compared with the results of angiography regionally.

2.7 Comparison with myocardial perfusion SPECT

Regions were divided into two parts as the decrease of reversible blood flow. All regions were selected according to the stenosis score(>50%) of angiography. Regional flow reserve (stress MBF - rest MBF) were analyzed in each part, respectively.

3 Results

3.1 Quantification of rMBF using ensemble ICA

Myocardium independent component images could be obtained in 15 among 20 subjects (see Fig. 2). The 5 subjects were excluded due to out of range (2 cases), imaging failure in stress (2 cases) and low SNR for analysis (1 case). Image contrast of myocardium was $1:2.97$ (LV:myocardium) in rest image, $1:2.56$ in stress image of separated independent component images. The number of subjects with the image contrast under 2.0 was 6, and the highest value of image contrast was 4.63. Blood flow obtained from PET was $1.2 \pm 0.40 ml/min/g$ in rest state, $1.85 \pm 1.12 ml/min/g$ in stress state. Reproducibility of myocardial blood flow of 15 subjects PET image data which were acquired twice for each region was high ($r = 0.99$ and $p < 0.0001$ where r is the correlation coefficient by paired t-test and p represents p-value which reflects statistical significance)

3.2 Analysis of PET blood flow as the result of angiography

A total of 83 segments from 9 patients who underwent coronary angiography were analyzed (see Figs. 3 and 4). According to angiography findings, 17 segments were classified into normal segments group, and 66 segments into stenotic segments group. The rMBF of normal segments which was measured by water PET was $1.16 \pm 0.36 ml/min/g$ in rest, $3.15 \pm 1.15 ml/min/g$ in stress. Blood flow reserve of normal segments group was $2.00 \pm 1.05 ml/min/g$. 66 segments were classified into stenotic segments group.

The rMBF of stenotic segments group was $1.06 \pm 0.37 ml/min/g$ in rest, $1.97 \pm 1.21 ml/min/g$ in stress, and blood flow reserve was $0.91 \pm 1.62 ml/min/g$. The blood flow reserve of stenotic segments group was significantly lower than normal segments group ($p < 0.05$). Myocardial perfusion was quantified by autoQuant program. Uptake value of normal segments group were $67.6 \pm 13.3\%$ in rest and $65.7 \pm 12.3\%$ in stress (reversibility score = 1.9), while that of stenotic

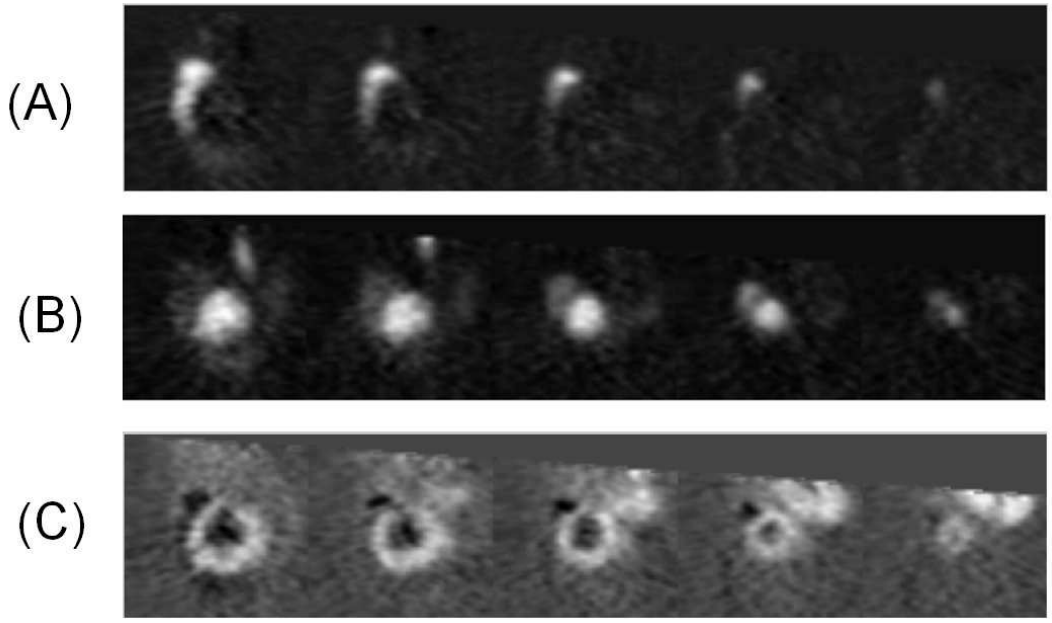

Figure 2: Independent component images from 60-year-old male with triple vessel disease. Short axis image of (A) (B) (C) from base to apex were displayed associated with cardiac components: (A) right ventricle; (B) left ventricle; (C) myocardium.

group were $71.9 \pm 9.8\%$ in rest and $69.1 \pm 12.8\%$ in stress (reversibility score =2.8). There was no significant difference between normal group and stenotic group in terms of reversibility score.

3.3 Comparison of MBF by myocardial perfusion SPECT and PET

We analyzed rMBF according to uptake value of myocardial perfusion SPECT. Among 66 stenotic segments, 19 segments showed high reversibility score (> 7, reversible segments), and 45 segments showed low reversibility score (≤ 7, persistent segment) in myocardial perfusion SPECT. The rMBF of reversible segments were $0.98 \pm 0.30 ml/min/g$ in rest, $1.78 \pm 0.76 ml/min/g$ in stress, and blood flow reserve was $0.80 \pm 0.69 ml/min/g$. The rMBF of persistent segments in myocardial perfusion SPECT was $1.10 \pm 0.40 ml/min/g$ in rest, $2.06 \pm 1.35 ml/min/g$ in stress, and blood flow reserve was $0.95 \pm 1.32 ml/min/g$. The blood flow reserve of reversible segments

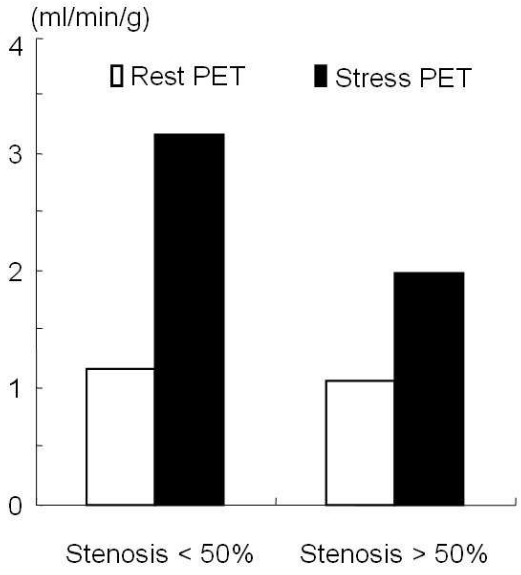

Figure 3: Absolute myocardial blood flow values measured using $H_2^{15}O$ PET at rest and during stress according to stenosis states. Perfusion reserve (stress blood flow - rest blood flow) was significantly different between the segments with and without stenosis ($p < 0.01$).

was tended to be lower than that of persistent segments, but $p > 0.05$ there was no statistical significance.

4 Conclusions

Various efforts have been made to separate cardiac components from dynamic $H_2^{15}O$ heart PET images [1, 17, 15]. In earlier study, we have successfully separated independent components in the animal study (dogs) using micro sphere and the natural gradient ICA method. However, major cardiac components were difficult to be extracted from clinical PET data by the conventional ICA, because of the difference of injection dose according to weight and low sensitivity of hardware system. Recently, left ventricle and myocardium images were visualized by NMF in the case of clinical patients' data. The MBF of patients could be estimated using NMF

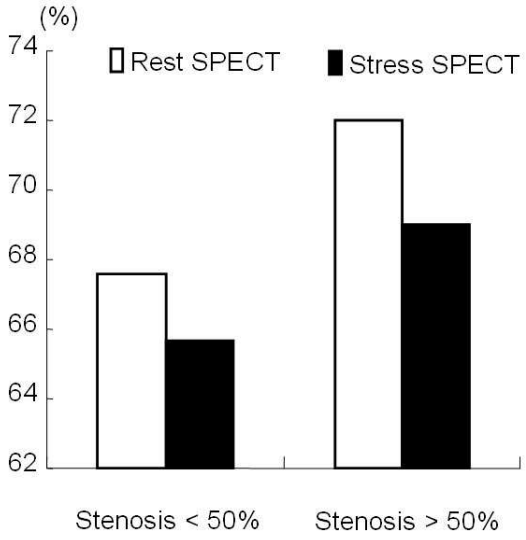

Figure 4: Correlation of relative myocardial uptake measured using ^{99m}Tc-MIBI SPECT and stenosis state. There was no significant difference in SPECT perfusion reversibility score between segment with stenosis and that without stenosis.

[15, 10, 16, 5], showing that the nonnegativity constraints are appropriate for nuclear science image analysis. However, the contrast and image quality were still not satisfactory enough to draw ROI on myocardium [15, 10].

Ensemble ICA allows us to impose nonnegativity constraints as well as independence conditions, on latent variables, leading to more flexible data fitting. We have applied ensemble ICA to the clinical PET data, showing that the image contrast and quality were improved for ROI processing, compared to NMF (see Fig. 5). Myocardial blood flow distribution obtained in this study corresponded to the known distribution [7, 9, 21, 5, 20, 2, 13].

We have shown that myocardial blood flow could be measured in a non-invasive manner from the time-activity curve of left ventricle and myocardium in $H_2^{15}O$ dynamic cardiac PET. We have demonstrated that rMBF measured by water PET could be applied to assess absolute myocardial blood flow. Flow reserve measured by water PET was significantly decreased in angiographically

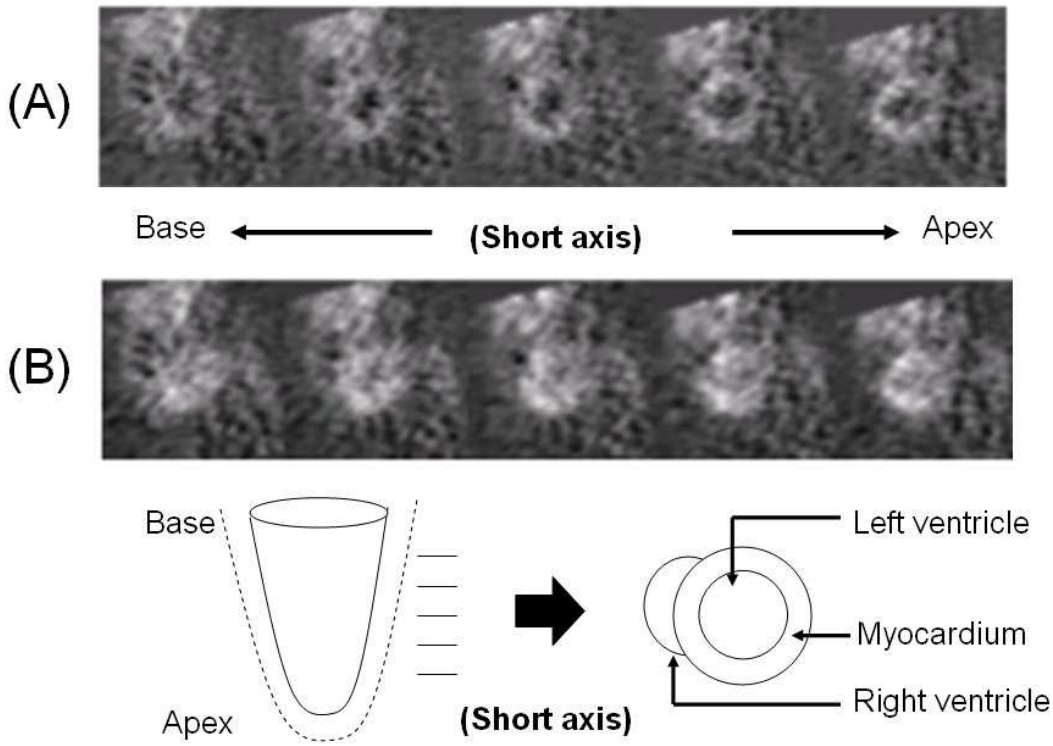

Figure 5: Component images associated with myocardium, that are computed from PET images taken from a 57-year-old female patient with coronary artery disease, are shown in the case of ensemble ICA (A) and NMF (B). Image contrast is improved using ensemble ICA, compared to NMF. Pictorial illustration in the bottom, where short axis images of heart from base to apex are displayed, depicts simplified cardiac components such as right ventricle, left ventricle, and myocardium, in order to emphasize that myocardial component images computed by ensemble ICA in this case clearly shows its structure, compared to ones determined by NMF.

stenotic segments compared with normal segments. However, myocardial perfusion SPECT did not show such difference of reversibility score between stenotic and normal segments, which is thought to be due to limitation of relative uptake. Our results were correlated with well-known findings that PET is a better method to assess myocardial perfusion than myocardial perfusion SPECT. In conclusion, rMBF was estimated using ensemble ICA in $H_2^{15}O$ dynamic myocardial

PET. We suggest that ensemble ICA incorporating non-negative constraint is a feasible method to handle dynamic image sequence obtained by the nuclear medicine techniques. Reproducibility of measurement and image contrast were good enough to segment myocardium. We expect that dynamic myocardial PET analysis using ensemble ICA can be used to assess absolute myocardial blood flow in clinical situations.

5 Acknowledgments

Authors would like to thank anonymous reviewers for their critical and valuable comments. This work was supported by KOSEF 2000-2-20500-009-5.

References

[1] J. Y. Ahn, D. S. Lee, J. S. Lee, S. K. Kim, G. J. Cheon, J. S. Yeo, and *et al.*, "Quantification of regional myocardial blood flow using H_2^{15} PET and factor analysis," *Journal of Nuclear Medicine*, vol. 42, pp. 782–787, 2001.

[2] P. Chareonthaitawee, P. A. Kaufmann, O. Rimoldi, and P. G. Camici, "Heterogeneity of resting and hyperemic myocardial blood flow in healthy humans," *Cardiovascular Research*, vol. 50, pp. 151–161, 2001.

[3] S. Choi, A. Cichocki, H. M. Park, and S. Y. Lee, "Blind source separation and independent component analysis: A review," *Neural Information Processing - Letters and Review*, vol. 6, no. 1, pp. 1–57, 2005.

[4] A. Cichocki and S. Amari, *Adaptive Blind Signal and Image Processing: Learning Algorithms and Applications*. John Wiley & Sons, Inc., 2002.

[5] K. H. Hwang, D. S. Lee, B. I. Lee, J. S. L. H. Y. Lee, J. K. Chung, and *et al.*, "Evaulation of endothelium-dependent myocardial perfusion reserve in healthy smokers: Cold pressor test using $H_2^{15}O$ PET," *Korean Journal of Nuclear Medicine*, vol. 38, pp. 21–29, 2004.

[6] A. Hyvärinen, J. Karhunen, and E. Oja, *Independent Component Analysis*. John Wiley & Sons, Inc., 2001.

[7] H. Iida, I. Kanno, A. Takahashi, and *et al.*, "Measurement of absolute myocardial blood flow with $H_2^{15}O$ and dynamic positron emission tomography strategy for qualification in relation to the partial volume effect," *Circulation*, vol. 78, pp. 104–115, 1998.

[8] H. Iida, Y. Tamura, K. Kitamura, P. M. Bloomfield, S. Eberl, and Y. Ono, "Histochemical correlates of ^{15}O-water-perfusable tissue fraction in experimental canine studies of old myocardial infraction," *Journal of Nuclear Medicine*, vol. 41, pp. 1737–1745, 2000.

[9] P. A. Kaufmann, T. Gnecchi-Ruscone, J. T. Yap, O. Rimoldi, and P. G. Camici, "Assessment of the reproducibility of baseline and hyperemic myocardial blood flow measurements with ^{15}O-labeled water and PET," *Journal of Nuclear Medicine*, vol. 40, pp. 1848–1856, 1999.

[10] S. K. Kim, S. Choi, B. I. Lee, K. H. Hwang, J. S. Lee, and D. S. Lee, "Improved visualization of dynamic $H_2^{15}O$ PET using NMF," *Korean Journal of Nuclear Medicine*, vol. 36, 2002.

[11] B. I. Lee, J. S. Lee, D. S. Lee, and S. Choi, "Myocardial blood flow quantification in dynamic PET: An ensemble ICA approach," in *Proc. Int'l Conf. Artificial Neural Networks*. Warsaw, Poland: Springer, 2005, pp. 709–714.

[12] D. D. Lee and H. S. Seung, "Learning the parts of objects by non-negative matrix factorization," *Nature*, vol. 401, pp. 788–791, 1999.

[13] D. S. Lee, K. W. Kang, K. H. Lee, J. M. Jeong, C. Kwark, and J. K. Chung, "Stress/Rest Tc-99m-MIBI SPECT in comparison with Rest/Stress rubidium-82 PET," *Korean Journal of Nuclear Medicine*, vol. 29, pp. 31–40, 1995.

[14] J. S. Lee, D. D. Lee, S. Choi, and D. S. Lee, "Application of non-negative matrix factorization to dynamic positron emission tomography," in *Proc. ICA*, San Diego, California, 2001, pp. 629–632.

[15] J. S. Lee, D. D. Lee, S. Choi, K. S. Park, and D. S. Lee, "Nonnegative matrix factorization of dynamic images in nuclear medicine," in *IEEE Medical Imaging Conference*, 2001.

[16] J. S. Lee and D. S. Lee, "Measurement of myocardial and cerebral blood flow using ^{15}O water," *Korean Journal of Nuclear Medicine*, vol. 35, pp. 43–51, 2001.

[17] J. S. Lee, D. S. Lee, J. Y. Ahn, S. K. Kim, G. J. Cheon, J. S. Yeo, K. S. Park, J. K. Chung, and M. C. Lee, "Blind separation of cardiac components and extraction of input function from $H_2^{15}O$ dynamic myocardial PET using independent component analysis," *Journal of Nuclear Medicine*, vol. 42, no. 6, pp. 938–943, 2001.

[18] J. S. Lee, K. S. Park, D. S. Lee, C. W. Lee, J. K. Chung, and M. C. Lee, "Development and applications of a software for functional image registration (FIRE)," *Computer Methods and Programs in Biomedicine*, vol. 78, pp. 157–164, 2005.

[19] J. W. Miskin and D. J. C. MacKay, "Ensemble learning for blind source separation," in *Independent Component Analysis: Principles and Practice*, S. Roberts and R. Everson, Eds. Cambridge University Press, 2001, pp. 209–233.

[20] W. M. Schaefer, B. Nowak, H. J. Kaiser, K. C. K. S. Block, and J. V. Dahl, "Comparison of microsphere-equivalent blood flow (^{15}O-water PET) and relative perfusion (99m Tc-Tetrofosmin SPECT) in myocardium showing metabolism-perfusion mismatch," *Journal of Nuclear Medicine*, vol. 44, pp. 33–39, 2003.

[21] K. P. Schäfers, T. J. Spinks, P. G. Camici, P. M. B. C. G. Rhodes, and M. P. Law, "Absolute quantification of myocardial blood flow with $H_2^{15}O$ and 3-dimensional PET: An experimental validation," *Journal of Nuclear Medicine*, vol. 43, pp. 1031–1040, 2002.